

# Electrochemically Controlling Ligand Binding Affinity for Transition Metals via RHLs: The Importance of Electrostatic Effects<sup>†</sup>

Alan M. Allgeier,<sup>‡</sup> Caroline S. Slone,<sup>‡</sup> Chad A. Mirkin,<sup>\*,‡</sup> Louise M. Liable-Sands,<sup>§</sup> Glenn P. A. Yap,<sup>§</sup> and Arnold L. Rheingold<sup>§</sup>

Contribution from the Department of Chemistry, 2145 Sheridan Road, Northwestern University, Evanston, Illinois 60208, and Department of Chemistry, University of Delaware, Newark, Delaware 19716

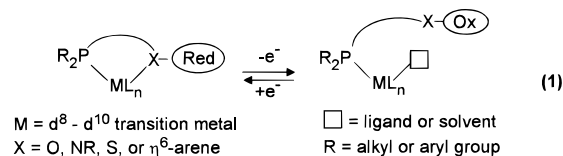
Received August 26, 1996<sup>⊗</sup>

**Abstract:** A series of redox-switchable hemilabile ligands (RHLs) has been synthesized that incorporates ferrocene as the redox group and phosphine ether or phosphine thioether moieties as binding groups. These ligands, which complex to Rh(I) and Pd(II), yield electrochemical control over ligand binding affinity for transition metals in complexes of the following type:  $[M(\eta^4-(\eta^5-C_5H_4XCH_2CH_2PR_2)_2Fe)]^{y+}$  (**5**: M = Rh, X = O, R = Ph (phenyl), y = 1; **6**: M = Rh, X = O, R = Cy (cyclohexyl), y = 1; **9**: M = Rh, X = S, R = Ph, y = 1; **10**: M = Pd, X = O, R = Ph, y = 2; **11**: M = Pd, X = O, R = Cy, y = 2). In the case of **11**, ligand based oxidation decreases the ligand to metal binding constant by nearly ten orders of magnitude. An examination of the crystal structures of **5**, **9**, **10**, and **11** and the electrochemical behavior of a series of RHL-complexes and isoelectronic model complexes reveals that electrostatic effects play a significant role in the charge dependent behaviors of these complexes. Additionally, there is a correlation between the phosphine substituents and RHL-complex stability. As a general rule cyclohexyl groups stabilize the complexes in their oxidized states over phenyl groups. In this study, RHLs are shown to provide a viable means of electrochemically controlling ligand binding affinity and thus the steric and electronic environment of bound transition metals.

## Introduction

We report the synthesis, characterization, and charge-dependent behavior of a series of transition metal complexes formed from redox-switchable hemilabile ligands (RHLs), Table 1. These ligands are designed to yield electrochemical control over ligand binding ability and thus the electronic and steric environment of a bound metal. Moreover, RHLs provide electrochemical control over the catalytic behavior and stoichiometric small molecule uptake and release properties of transition metal centers that are bound to them.<sup>1</sup>

A redox-switchable hemilabile ligand is a multidentate ligand with binding centers of various affinities for a transition metal, eq 1. For the examples in this study, the phosphine moiety



forms a strong bond to late transition metals and is substitutionally inert. The X groups in eq 1 (e.g., ethers in this study) form weaker interactions with the metal and may be displaced readily in the presence of stronger donating ligands such as acetonitrile (MeCN) or CO. The chemistry of hemilabile ligands, especially (P,O) ligands, has been thoroughly studied and applied extensively in homogeneous catalysis.<sup>2</sup> Central to

<sup>†</sup> Keywords: redox ligand, charge-dependent reactivity, hemilabile, phosphine ether ligand.

<sup>‡</sup> Northwestern University.

<sup>§</sup> University of Delaware.

<sup>⊗</sup> Abstract published in *Advance ACS Abstracts*, January 1, 1997.

(1) Slone, C. S.; Mirkin, C. A. Manuscript in preparation.

(2) For a review, see: Bader, A.; Lindner, E. *Coord. Chem. Rev.* **1991**, 108, 27.

**Table 1.** NMR Data for Tetradentate RHLs and Their Metal Complexes

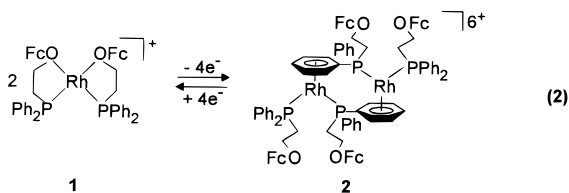
				<sup>1</sup> H Fc	<sup>31</sup> P( <i>J</i> <sub>Rh-P</sub> , Hz)	solvent
<b>3a</b>	X = O	M = none	R = Ph	3.92, 3.66	-21.9	C <sub>6</sub> D <sub>6</sub>
<b>3b</b>	X = O	M = none	R = Cy	4.05, 3.81	-11.1	CDCl <sub>3</sub>
<b>3c</b>	X = S	M = none	R = Ph	4.26, 4.21	-16.6	CDCl <sub>3</sub>
<b>5</b>	X = O	M = Rh(I)	R = Ph	4.75, 4.10	61.1 (210)	CD <sub>2</sub> Cl <sub>2</sub>
<b>6</b>	X = O	M = Rh(I)	R = Cy	4.63, 4.04	68.3 (203)	CD <sub>2</sub> Cl <sub>2</sub>
<b>9</b>	X = S	M = Rh(I)	R = Ph	4.84, 4.34	62.7 (162)	CD <sub>2</sub> Cl <sub>2</sub>
<b>10</b>	X = O	M = Pd(II)	R = Ph	5.22, 4.09	51.3	CD <sub>2</sub> Cl <sub>2</sub>
<b>11</b>	X = O	M = Pd(II)	R = Cy	4.94, 4.10	72.9	CD <sub>2</sub> Cl <sub>2</sub>

the design of RHLs is the placement of an electroactive group in electronic communication with the weakly binding center. Upon oxidation of the redox group, an inductive withdrawal of electron density weakens the M–X interaction and, in some cases, may lead to dissociation of the labile X functionality, eq 1.<sup>3</sup> For cationic transition metal complexes (e.g., M = Rh(I) or Pd(II)) formed from neutral RHLs this effect will be exacerbated when oxidation of the redox group generates a cationic center and thus establishes electrostatic repulsion between the central metal and the newly formed cationic center. In principle, the magnitude of the effects may be tailored by altering the RHL phosphine substituents, varying the weakly binding center (e.g.,

(3) (a) Singewald, E. T.; Mirkin, C. A.; Stern, C. L. *Angew. Chem., Int. Ed. Engl.* **1995**, 34, 1624. (b) Sassano, C. A.; Mirkin, C. A. *J. Am. Chem. Soc.* **1995**, 117, 11379. (c) For a related approach using proton-coupled *p*-quinonyl redox chemistry, see: Sembring, S. B.; Colbran, S. B.; Craig, D. C. *Inorg. Chem.* **1995**, 34, 761.

ether, thioether, amine,  $\eta^6$ -arene,<sup>3b,4</sup> etc.) and controlling the distance separating the redox group and the central metal.

Previous work in our laboratories has illustrated the utility of RHLs for controlling the coordination environments of bound transition metals.<sup>3</sup> Upon ligand based oxidation, square planar complex **1** undergoes an unprecedented, electrochemically-induced haptotropic rearrangement to form the 36 electron dimeric complex, **2** with each Rh in a piano stool geometry, eq 2.<sup>3a</sup> Significantly, the entire four-electron process is chemically



reversible, which suggests the possibility of using RHLs to electrochemically generate multiple states of catalytic activity in a reversible fashion.

Substitutionally inert ligands containing electroactive groups have been utilized for controlling the properties and reactivity of bound transition metals.<sup>5</sup> In an approach fundamentally different from the one described herein, the oxidation of a *substitutionally inert* redox-active ligand bound to a transition metal has been used to alter a complex's chemical and physical properties.<sup>5</sup> Indeed, using such a strategy, the rates of stoichiometric reactions have been accelerated by factors as large as 5400,<sup>5b</sup> while catalytic reactions exhibit more modest rate enhancements.<sup>5a</sup> Others have exploited reduction of a bound metal as a means of altering the ligand environment of metal complexes containing redox-inactive ligands.<sup>6</sup> Still other researchers have designed molecular redox switches for the controlled binding of hard metal ions,<sup>7</sup> predominantly those from Groups I and II of the Periodic Table. Many of these ligands are designed to reversibly complex alkali and alkaline earth metal cations as a function of the ligand's state of charge. Oxidation of these systems, which are predominantly ferrocenyl crown ethers<sup>7h,i</sup> and aza-crown ethers,<sup>7a,c,e,f,j</sup> typically results in a substantial decrease in crown binding constant for the cationic guest.<sup>7c,e-j</sup>

Studies focusing on redox-switches based upon crown ethers or aza-crown ethers and alkali or alkaline earth metal cations

(4) Singewald, E. T.; Shi, X.; Mirkin, C. A.; Schofer, S. J.; Stern, C. L. *Organometallics* **1996**, *15*, 3062.

(5) (a) Lorkovic, I. M.; Duff, R. R., Jr.; Wrighton, M. S. *J. Am. Chem. Soc.* **1995**, *117*, 3617. (b) Lorkovic, I. M.; Wrighton, M. S.; Davis, W. M. *J. Am. Chem. Soc.* **1994**, *116*, 6220. (c) Miller, T. M.; Ahmed, K. J.; Wrighton, M. S. *Inorg. Chem.* **1989**, *28*, 2347. (d) Kotz, J. C.; Nivert, C. L.; Lieber, J. M.; Reed, R. C. *J. Organomet. Chem.* **1975**, *91*, 87. (e) Kotz, J. C.; Nivert, C. L. *J. Organomet. Chem.* **1973**, *52*, 397. (f) Yeung, L. K.; Kim, J. E.; Chung, Y. K.; Rieger, P. H.; Sweigart, D. A. *Organometallics* **1996**, *15*, 3891.

(6) (a) Kuchynka, D. J.; Kochi, J. K. *Inorg. Chem.* **1988**, *27*, 2574. (b) Hershberger, J. W.; Kochi, J. K. *J. Chem. Soc., Chem. Commun.* **1982**, 212. (c) Bowyer, W. J.; Merkert, J. W.; Geiger, W. E.; Rheingold, A. L. *Organometallics* **1989**, *8*, 191.

(7) For representative examples, see: (a) Plenio, H.; Yang, J.; Diodone, R.; Heinze, J. *Inorg. Chem.* **1994**, *33*, 4098. (b) Kim, J. S.; Bessire, A. J.; Bartsch, R. A.; Holwerda, R. A.; Czech, B. P. *J. Organomet. Chem.* **1994**, *484*, 47. (c) Medina, J. C.; Goodnow, T. T.; Rojas, M. T.; Atwood, J. L.; Lynn, B. C.; Kaifer, A. E.; Gokel, G. W. *J. Am. Chem. Soc.* **1992**, *114*, 10583. (d) Beer, P. D.; Nation, J. E.; Harman, M. E.; Hursthouse, M. B. *J. Organomet. Chem.* **1992**, *441*, 465. (e) Beer, P. D.; Keefe, A. D.; Sikanyika, H.; Blackburn, C.; McAleer, J. F. *J. Chem. Soc., Dalton Trans.* **1990**, 3289. (f) Hall, C. D.; Sharpe, N. W.; Danks, I. P.; Sang, Y. P. *J. Chem. Soc., Chem. Commun.* **1989**, 419. (g) Echegoyan, L. E.; Yoo, H. K.; Gatto, V. J.; Gokel, G. W.; Echegoyan, L. *J. Am. Chem. Soc.* **1989**, *111*, 2440. (h) Beer, P. D. *Chem. Soc. Rev.* **1989**, *18*, 409. (i) Saji, T. *Chem. Lett.* **1986**, 275. (j) Shinkai, S.; Inuzurka, K.; Miyazake, O.; Manabe, O. *J. Am. Chem. Soc.* **1985**, *107*, 3950. (k) Hall, C. D.; Chu, S. Y. F. *J. Organomet. Chem.* **1995**, *498*, 221.

have shown that electrostatic repulsion between the oxidized ligand and the sequestered cation substantially contributes to the oxidation-state dependent binding ability of these electrochemically active sequestering agents.<sup>7c,e-j</sup> For alkali and alkaline earth metals, electrostatic repulsion is a significant factor contributing to the destabilization of the coordination sphere, since such metals have high charge densities. In contrast, a transition metal has the ability to delocalize its charge upon ancillary ligands; the amount of delocalization is highly dependent on the transition metal and the types of ancillary ligands that comprise a complex. Therefore, the true ionic nature of a transition metal ion is not easily predicted. For instance, d<sup>8</sup> Ir or Rh complexes are referred to as both containing cationic electrophilic metal centers and "electron rich" nucleophilic metal centers. Indeed, some d<sup>8</sup> Ir complexes act as Lewis bases by binding Lewis acids like BF<sub>3</sub>.<sup>8</sup> In the design of RHL-transition metal complexes, a key issue pertains to the significance of electrostatic effects in the destabilization of the transition metal coordination sphere upon ligand oxidation. Increased destabilization that results from moving a complex from one oxidation state to the next should yield a greater change in complex reactivity. Herein, we describe a systematic study aimed at determining the importance of electrostatic effects in RHL-transition metal complexes and, more importantly, how those effects can be maximized through the positioning of the redox-active portion of the RHL, choice of transition metal, and choice of phosphine substituents.

To probe the importance of electrostatic effects in controlling RHL-transition metal behavior through RHL oxidation state, tetradentate **3a-c** were designed and synthesized for complexation to late transition metals, Table 1. In addition to structural rigidity, these RHLs offer one the ability to tune the electronic nature of the complexed metal by varying the phosphine substituents or replacing the ether moiety with other weakly binding groups. The impact of these variations upon RHL-metal complex behavior provides a basis upon which to understand and rationally design RHL systems. Changing the valency of the bound metal allows one to draw a correlation between transition metal charge density and complex stability in the oxidized and reduced states. Additionally, comparing the behavior of metal complexes of **3** with less constrained complexes such as **1**, eq 2, gives insight into the role of electrostatic interactions in the destabilization of RHL metal complexes. Through an examination of a series of RHL transition metal complexes, the work presented herein allows one to assess the usefulness of RHLs in altering transition metal reactivity, and it provides insight into the factors that control the magnitudes of these interesting and potentially useful ligand based effects.

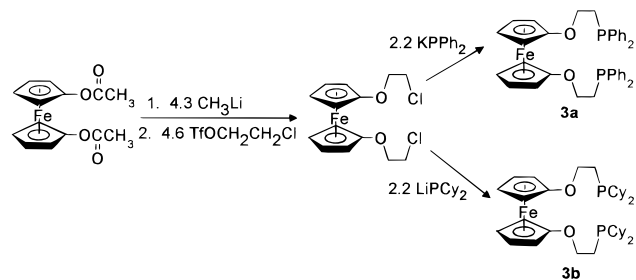
## Results and Discussion

**Synthesis and Structure.** Ferrocene is a well-studied compound<sup>9</sup> that is stable in two oxidation states and, therefore, an attractive synthetic building block for RHLs. Among the many derivatives of ferrocene, those with heteroatoms directly bonded to the cyclopentadienyl (Cp) rings often are the most synthetically challenging. Ligands **3a,b**, which contain ferrocenyl ether linkages, were prepared via Williamson ether syntheses, as outlined in Scheme 1. Deprotection of ferrocenylene diacetate with methyllithium provided the corresponding dialkoxide,<sup>10</sup> which was subsequently reacted with 2-chloro-

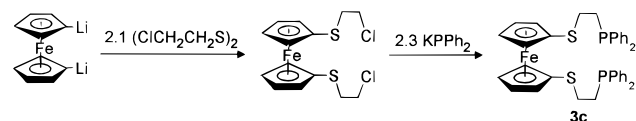
(8) Scott, R. N.; Shriver, D. F.; Lehman, D. D. *Inorg. Chim. Acta* **1970**, *4*, 73.

(9) Rosenblum, M. *Chemistry of the Iron Group Metallocenes*; Interscience: New York, 1965.

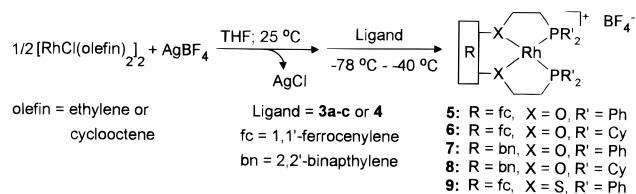
## Scheme 1



## Scheme 2



## Scheme 3



ethyltrifluoromethane sulfonate.<sup>11</sup> The alkyl triflate was chosen as the electrophile to avoid cyclization to 1,4-dioxo[4]-ferrocenophane,<sup>12</sup> while leaving an alkyl chloride available for further reaction. The alkyl chloride was displaced by the desired phosphide nucleophile to provide **3a,b**, which were purified by column chromatography and isolated as orange microcrystalline solids. The ligands have been spectroscopically characterized, and all data are consistent with the proposed structures, Table 1.

There has been recent interest in the synthesis of sulfur substituted ferrocene groups,<sup>13</sup> and such precedent has provided a synthetic pathway to thioether RHLs. The phosphine thioether **3c** was synthesized via an analogous literature method for forming ferrocenyl sulfides.<sup>13a</sup> The synthesis begins by reacting 1,1'-dilithioferrocene with 2-chloroethyldisulfide<sup>14</sup> yielding 1,1'-bis(2-chloroethylthio)ferrocene,<sup>15</sup> Scheme 2. Nucleophilic displacement of the chloride groups with potassium diphenylphosphide provides ligand **3c** as an orange microcrystalline solid. In the course of this study it was necessary to examine the behavior of model complexes based on ligands **4a**<sup>16</sup> and **4b**, Table 2; the latter was synthesized in a manner directly analogous to the literature method for preparing **4a**.<sup>16</sup>

In anticipation of future investigations pertaining to the catalytic behavior of complexes formed from ligands **3-4**, we chose to study their d<sup>8</sup> metal complexes. We have previously communicated the complexation of **3a** to Rh(I) to form **5** (Table 1) and compound **5**'s behavior as an olefin hydrogenation

(10) Nesmeyanov, A. N.; Sazonova, V. A.; Drozd, V. N.; Nikonova, L. A. *Dokl. Akad. Nauk. SSSR (Engl. Transl.)* **1960**, *133*, 751; *Dokl. Akad. Nauk. SSSR* **1960**, *133*, 126.

(11) Katsuhara, Y.; Desmarteau, D. D. *J. Fluorine Chem.* **1980**, *16*, 257.

(12) Akabori, S.; Habata, Y.; Sakamoto, Y.; Sato, M.; Ebine, S. *Bull. Chem. Soc. Jpn.* **1983**, *56*, 537.

(13) (a) McCulloch, B.; Ward, D. L.; Woolins, J. D.; Brubaker, C. H. Jr. *Organometallics* **1985**, *4*, 1425. (b) Brandt, P. F.; Rauchfuss, T. B. *J. Am. Chem. Soc.* **1992**, *114*, 1927.

(14) For the original synthesis of 2-chloroethyldisulfide, see: Vilsmaier, E.; Sprügel, W. *Liebigs Ann. Chem.* **1971**, *749*, 62.

(15) 1,1'-Bis(2-chloroethylthio)ferrocene has been reported previously in the literature, but it was synthesized by a different route. See: Sato, M.; Tanaka, S.; Ebine, S.; Akabori, S. *Bull. Chem. Soc. Jpn.* **1984**, *57*, 1929.

(16) Higgins, T. B.; Mirkin, C. A. *Inorg. Chim. Acta* **1995**, *240*, 347.

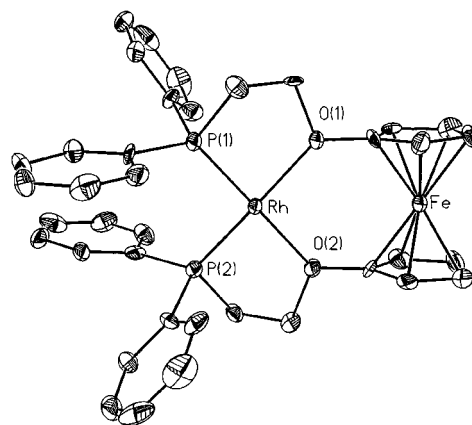
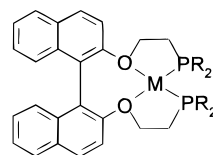


**Figure 1.** Molecular structure of **5**. Ellipsoids are drawn at 50% probability. Selected bond distances and angles: Rh–Fe: 3.992(2) Å, Rh–O1: 2.195(7) Å, Rh–O2: 2.185(7) Å, Rh–P1: 2.156(3) Å, Rh–P2: 2.163(3) Å. O1–Rh–O2: 97.8(3)°, O2–Rh–P2: 83.3(2)°, P2–Rh–P1: 96.2(1)°, P1–Rh–O1: 82.7(2)°.

**Table 2.** NMR Data for Model Ligands and Their Metal Complexes



			<sup>31</sup> P ( <i>J</i> <sub>Rh,P</sub> , Hz)	solvent
<b>4a</b>	M = none	R = Ph	–22.4	C <sub>6</sub> D <sub>6</sub>
<b>4b</b>	M = none	R = Cy	–10.8	CDCl <sub>3</sub>
<b>7</b>	M = Rh(I)	R = Ph	63.2 (212)	CD <sub>2</sub> Cl <sub>2</sub>
<b>8</b>	M = Rh(I)	R = Cy	72.6 (203)	CD <sub>2</sub> Cl <sub>2</sub>

catalyst.<sup>17</sup> Ligands **3-4** all complex Rh(I) in an analogous manner, Scheme 3. Chloride abstraction from a Rh(I)-chloro-olefin dimeric or polymeric complex with AgBF<sub>4</sub>, followed by the addition of 1 equiv of tetradentate ligand (**3-4**) at low temperature, gives Rh(I) *cis*-ether *cis*-phosphine complexes in moderate to high isolated yields. The complexes exhibit large downfield shifts in their <sup>31</sup>P NMR spectra, which are characteristic of phosphines in five membered chelate rings,<sup>18</sup> Tables 1 and 2. Interestingly, other Rh(I) *cis*-ether *cis*-phosphine complexes have been reported in the literature to be unstable above –30 °C.<sup>18c</sup> Although complexes **5** and **6-8** (Tables 1 and 2) are very reactive species, especially with oxygen, they are not inherently unstable at room temperature in CH<sub>2</sub>Cl<sub>2</sub> solution or in the solid-state under very pure conditions. This enhanced stability is, likely, a result of the chelating ability of these tetradentate ligands.

Orange crystals of **5**·THF (THF = tetrahydrofuran) were grown from slow diffusion of pentane into THF, and they provide the first known example of a crystallographically characterized Rh(I) complex with a ligand array comprised exclusively of phosphine ether ligands, Figure 1. For the sake of simplicity, the cation of **5**·THF will be referred to as **5**. Compound **5** has distorted square-planar geometry around Rh with an average Rh–O distance of 2.19 Å, which compares

(17) Allgeier, A. M.; Singewald, E. T.; Mirkin, C. A.; Stern, C. L. *Organometallics* **1994**, *13*, 2928.

(18) (a) Garrou, P. E. *Chem. Rev.* **1981**, *81*, 229. (b) Lindner, E.; Wang, Q.; Mayer, H. A.; Fawzi, R.; Steimann, M. *J. Organomet. Chem.* **1993**, *453*, 289. (c) Lindner, E.; Andres, B. *Chem. Ber.* **1987**, *120*, 761. (d) Brown, J. M.; Cook, S. J.; Kent, A. G. *Tetrahedron* **1986**, *42*, 5097. (e) Lindner, E.; Wang, Q.; Mayer, H. A.; Fawzi, R.; Steimann, M. *Organometallics* **1993**, *12*, 1865.

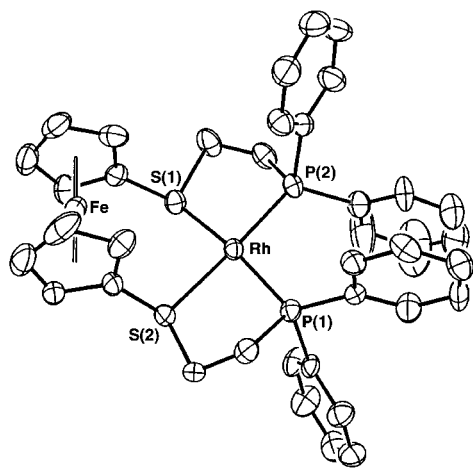


**Figure 2.** An ORTEP diagram of **9**. Ellipsoids are drawn at 50% probability. Selected bond distances and angles: Rh–Fe: 4.055(7) Å, Rh–S1: 2.326(3) Å, Rh–S2: 2.349(2) Å, Rh–P1: 2.241(2) Å, Rh–P2: 2.236(3) Å. S1–Rh–S2: 89.34(9)°, S2–Rh–P1: 85.37(9)°, P1–Rh–P2: 98.98(9)°, P2–Rh–S1: 86.10(9)°.

well with the average literature value for Rh–O bond lengths (2.22 Å)<sup>18b,e,19</sup> in complexes with phosphine ether ligands. The average Rh–P distance of 2.16 Å in **5** is somewhat shorter than the average Rh–P bond (2.26 Å)<sup>18b,e,19</sup> for literature complexes containing phosphine ether ligands. The nature of this disparity is not well understood. The Rh–Fe distance in **5** is 3.992(2) Å and will be a significant parameter in the analysis of its electrochemical behavior. The O(1)–Rh–P(1) and O(2)–Rh–P(2) angles are compressed (average = 83.0°) as compared with the O(1)–Rh–O(2) angle of 97.8(3)° and the P(1)–Rh–P(2) angle of 96.2(1)°. The relatively large O(1)–Rh–O(2) angle is a result of the O(1)–O(2) separation in **5**, which is dictated by the cyclopentadienyl rings of the ferrocenyl moiety. In fact, the rigidity of the ferrocenyl group controls the geometry; another complex, which contains a bis-phosphine bis-ether ligand in the tetradentate binding mode around Rh(III), has a O–Rh–O angle of 79.1(3)°.<sup>19c</sup> The large P(1)–Rh–P(2) angle may be a consequence of steric crowding of the phenyl rings attached to P(1) and P(2). The two planes defined by the cyclopentadienyl ring carbons are parallel (dihedral angle = 2.37°) and separated by 3.3 Å. Although **5** crystallizes with one equiv of THF, there is no evidence in the solid state or in solution for a bonding interaction between the THF molecule and the Rh<sup>+</sup> center. High solvent affinity seems to be a property of complexes of this type (*vide infra*). The steric rigidity imposed by the ligand framework of **3** suggests that the Rh–Fe separation in **6** will be nearly the same as that in **5**.

Complex **9**, a thioether analogue to **5**, was crystallized from a mixture of THF and pentane. As with **5**, THF is present in crystals of **9** but only at 50% occupancy, and there is no indication of a bonding interaction between the THF molecule and the Rh complex. The cation in the structure of **9**·0.5 THF (for simplicity referred to as **9** hereon), Figure 2, bears strong resemblance to that of an isoelectronic Rh complex in the literature, [Rh( $\eta^2$ -Ph<sub>2</sub>PCH<sub>2</sub>CH<sub>2</sub>SCH<sub>3</sub>)<sub>2</sub>][BF<sub>4</sub>].<sup>20</sup> Bond distances and angles around Rh in these two complexes are very similar and compare well with bond distances of other literature

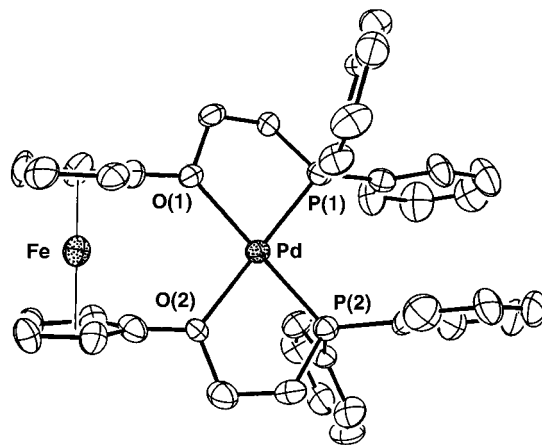
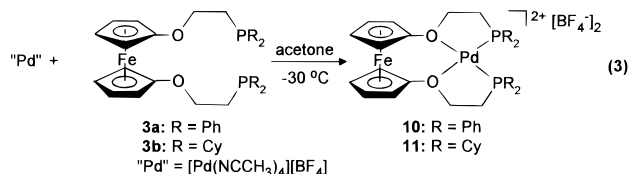


**Figure 3.** An ORTEP diagram of **10**. Ellipsoids are drawn at 50% probability. Selected bond distances and angles: Pd–Fe: 3.945(6) Å, Pd–O1: 2.163(7) Å, Pd–O2: 2.165(7) Å, Pd–P1: 2.222(3) Å, Pd–P2: 2.219(3) Å. O1–Pd–O2: 99.2(3)°, O2–Pd–P2: 82.1(2)°, P2–Pd–P1: 97.45(12)°, P1–Pd–O1: 81.4(2)°.

complexes containing thioether and phosphine ligands.<sup>21</sup> The Rh–Fe separation (4.055(7) Å) is slightly longer than that observed for **5** and is consistent with elongation in the Rh–S bonds (average = 2.34 Å) in **9**, as compared with the Rh–O bonds in **5**. To accommodate this elongation in the Rh–S bonds and to keep the ferrocenyl unit intact, the structure has a significantly smaller S(1)–Rh–S(2) angle (89.34(9)°) than the O(1)–Rh–O(2) angle of **5** (97.8(3)°). Note that these structural variations indicate that the ferrocenyl group dictates the rigidity of the chelate pocket.

Electrochemical studies, which are discussed later in this manuscript, led to the synthesis of palladium(II) analogues of **5** and **6**. As d<sup>8</sup> transition metals, Rh(I) and Pd(II) are expected to form complexes with similar structures. Indeed, reaction of [Pd(NCCH<sub>3</sub>)<sub>4</sub>][BF<sub>4</sub>]<sub>2</sub> with one equiv of **3a** or **3b** in acetone provides square planar complexes, **10** and **11**, respectively, eq 3. The Pd complexes yield spectroscopic data, consistent with their proposed structures, Table 1. Additionally, crystals of **10**·0.6 CH<sub>2</sub>Cl<sub>2</sub> and **11**, suitable for X-ray diffraction, were grown by slow diffusion of pentane or ether into methylene chloride



solutions. Note, **11** is the only compound in this series that does not crystallize with solvent. The molecular structures of the cations in both **10**·0.6CH<sub>2</sub>Cl<sub>2</sub> and **11** (referred to as **10** and **11** hereon, Figures 3 and 4) reveal square planar ligand arrangements around Pd with 0.06 Å and 0.05 Å average deviations from the O(1), O(2), P(1), P(2) planes, respectively. The structures are similar to an isoelectronic, square planar Pd-

(19) (a) Werner, H.; Hampp, A.; Peters, K.; Peters, E. M.; Walz, L.; von Schnering, H. G. *Z. Naturforsch., B: Anorg. Chem., Org. Chem.* **1990**, *45*, 1548. (b) Haefner, S. C.; Dunbar, K. R.; Bender, C. *J. Am. Chem. Soc.* **1991**, *113*, 9540. (c) Alvarez, M.; Lugan, N.; Mathieu, R. *J. Organomet. Chem.* **1994**, *468*, 249.

(20) Dick, D. G.; Stephan, D. W. *Can. J. Chem.* **1986**, *64*, 1870.

(21) (a) Blake, A. J.; Halcrow, M. A.; Schröder, M. *Acta Crystallogr.* **1993**, *C49*, 85. (b) Alvarez, M.; Lugan, N.; Mathieu, R. *Inorg. Chem.* **1993**, *32*, 5652. (c) Teixidor, R.; Rius, J.; Miravittles, C.; Viñas, C.; Escriche, L.; Sanchez, E.; Casabó, J. *Inorg. Chim. Acta* **1990**, *176*, 61. (d) Sellmann, D.; Fetz, A.; Moll, M.; Knoch, F. *Polyhedron* **1989**, *8*, 613. (e) Sellmann, D.; Fetz, A.; Moll, M.; Knoch, F. *J. Organomet. Chem.* **1988**, *355*, 495. (f) Bianchini, C.; Mealli, C.; Meli, A.; Sabat, M.; Silvestre, J.; Hoffmann, R. *Organometallics* **1986**, *5*, 1733. (g) Cheng, C.-H.; Eisenberg, R. *Inorg. Chem.* **1979**, *18*, 2438. (h) Cheng, C.-H.; Spivack, B. D.; Eisenberg, R. *J. Am. Chem. Soc.* **1977**, *99*, 3003.

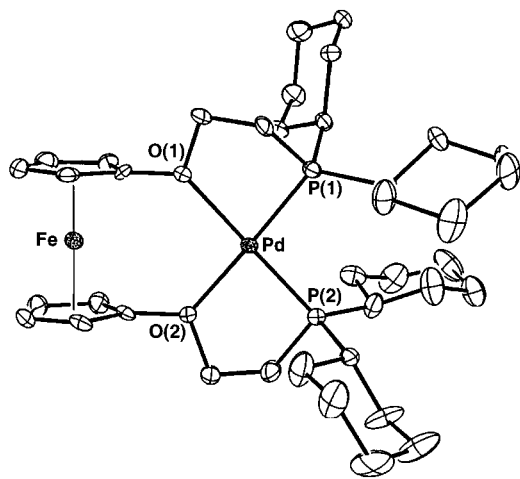


**Figure 4.** An ORTEP diagram of **11**. Ellipsoids are drawn at 50% probability. Selected bond distances and angles: Pd–Fe: 3.982(7) Å, Pd–O1: 2.179(4) Å, Pd–O2: 2.178(4) Å, Pd–P1: 2.231(2) Å, Pd–P2: 2.233(2) Å, O1–Pd–O2: 98.0(2)°, O2–Pd–P2: 84.48(12)°, P2–Pd–P1: 97.90(7)°, P1–Pd–O1: 80.68(12)°.

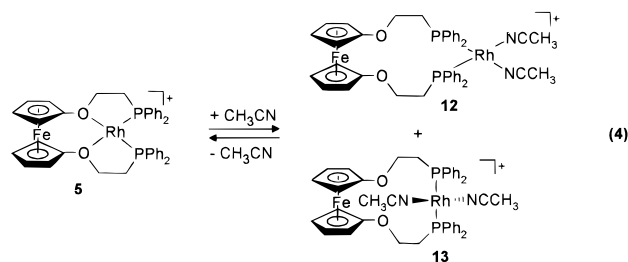
(II) complex in the literature<sup>22</sup> and bond distances around Pd have comparable values. For **10**, the average Pd–O distance is 2.16 Å, slightly shorter than the average Pd–O distance in **11** (2.18 Å). This difference is consistent with a weaker (and longer) Pd–O bond in **11** when compared with **10**, and it is a result of the “softer,” Cy<sub>2</sub>P-substituted Pd center in **11** forming a weaker interaction with the “hard” oxygen binding moieties. Other crystallographically characterized Pd complexes containing phosphine ether ligands have bond distances and angles similar to **10** and **11**.<sup>23</sup> As predicted, the ferrocenyl units are rigid, and the Cp rings are virtually planar; the angle between the Cp planes is 3.0° for **10** and 2.7° for **11**. The rigidity of the ferrocenyl unit imposes nearly constant Fe–M separations in **10** (3.945(6) Å) and **11** (3.982(7) Å), which are nearly equiv to the M–Fe separation in **5** (3.992(2) Å). Having this parameter fixed in this series of complexes will be essential in the evaluation of their electrochemical behavior.

**Spectroscopy and Reactivity.** Complexes **5–11** all exhibit diagnostic downfield chemical shifts in the <sup>31</sup>P NMR spectra relative to the free ligands, **3a–c** and **4a–b**, and complexes of isoelectronic monodentate ligands,<sup>18</sup> Tables 1 and 2. For instance, complex **5** exhibits a <sup>31</sup>P NMR shift at δ 61.1, while ligand **3a** exhibits a resonance at δ –21.9. Similarly, complex **6** exhibits a <sup>31</sup>P NMR shift at δ 68.3, while ligand **3b** exhibits a resonance at δ –11.1. Such shifts indicate the phosphine is one of a five-membered chelate ring; this phenomenon, which is general to transition metal phosphine complexes, has been reviewed in detail.<sup>18a</sup> For complexes **5–9**, since the Rh–P coupling constants are dictated by the ligands *trans* to the phosphines, the coupling constants observed in their <sup>31</sup>P NMR spectra provide further confirmation of their structures in solution. Notably, *J*<sub>Rh–P</sub> for the thioether complex, **9** (161 Hz), is significantly lower than the values corresponding to the ether complexes, **5–8**. All of the *cis*-ether *cis*-phosphine complexes exhibit coupling constants in the 203–212 Hz range, which is diagnostic of these types of complexes.<sup>16,18</sup> Similarly, the

coupling constant of **9** compares well with the few isoelectronic examples in the literature.<sup>20,24</sup>

The series of complexes **5**, **6** and **9–11** contain bound metals of varying electronic nature. The Pd(II) complexes are isoelectronic with their Rh(I) counterparts but more electron-withdrawing due to their greater formal charge. The electron withdrawing properties of these metal cations also are affected by phosphine substituents. The chemical shift values for the ferrocenyl α-hydrogens are the most diagnostic indicators of the relative electron withdrawing properties of the metal centers in these complexes. For instance in moving from **6** to **11**, the chemical shift increases from δ 4.63 to δ 4.94 (CD<sub>2</sub>Cl<sub>2</sub>), in accord with the increased electron withdrawing ability of Pd(II) when compared with Rh(I), Table 1. Likewise, the phenyl substituted complexes are more electron withdrawing than the cyclohexyl substituted complexes, as evidenced by the observation that **5** exhibits an α-ferrocenyl proton shift of δ 4.75, while the α-ferrocenyl protons of **6** resonate at δ 4.63. These trends of chemical shifts with electronic nature of the central metal hold true throughout the series of RHL compounds in this study. More than just being structurally informative, these trends indicate another level of control in RHL transition metal chemistry by varying the bound central metal and the phosphine substituents in RHL complexes one can tune the electronic nature of an RHL complex and thus alter its stability.

The hemilabile properties of **5** and **6** have been demonstrated in their reactivity studies with acetonitrile. In neat acetonitrile (MeCN-*d*<sub>3</sub>), compound **5** is converted to a 4:1 ratio of the *cis*- and *trans*-MeCN adducts, **12** and **13**, respectively, eq 4. This process, which demonstrates the lability of the Rh–ether linkages, may be reversed by the removal of solvent. Structural



assignments of **12** and **13** were made on the basis of <sup>1</sup>H and <sup>31</sup>P NMR spectroscopy. When compound **5** is dissolved in MeCN-*d*<sub>3</sub>, the <sup>31</sup>P NMR spectrum exhibits two resonances at δ 41.1 (*J*<sub>Rh–P</sub> = 172 Hz) and δ 19.9 (*J*<sub>Rh–P</sub> = 130 Hz). The *J*<sub>Rh–P</sub> values are diagnostic of the *cis*- and *trans*-square planar geometries of these complexes, respectively.<sup>4,18a,25</sup> Also consistent with this formulation, the <sup>1</sup>H NMR of **5** in CD<sub>2</sub>Cl<sub>2</sub> with excess MeCN exhibits a broad resonance at δ 1.87 which is assigned to Rh-coordinated MeCN (free MeCN: δ 1.98). Complex **6** also undergoes reaction with MeCN however, only the *trans* isomer **14** is formed. Even at low temperature (–50 °C) and when a large excess of MeCN (120 equiv) is present in a CD<sub>2</sub>Cl<sub>2</sub> solution of **6**, no *cis*-product is observed. Assignment of the geometry was made on the basis of the <sup>31</sup>P NMR data; a single resonance was observed at δ 31.8 with *J*<sub>Rh–P</sub> = 127 Hz. Again the coupling constant is diagnostic of the ligand *trans* to the phosphine. The difference in the product ratios for the reactions involving MeCN with **5** and **6** may be a consequence of increased steric bulk of the cyclohexyl groups

(22) Lindner, E.; Dettinger, J.; Fawzi, R.; Steimann, M. *Chem. Ber.* **1993**, *126*, 1347.

(23) (a) Dunbar, K. R.; Sun, J.-S. *J. Chem. Soc., Chem. Commun.* **1994**, 2387. (b) Tani, K.; Nakamura, S.; Yamagata, T.; Kataoka, Y. *Inorg. Chem.* **1993**, *32*, 5398. (c) Lindner, E.; Dettinger, J.; Mayer, H. A.; Kühbauch, H.; Fawzi, R.; Steimann, M. *Chem. Ber.* **1993**, *126*, 1317. (d) Lindner, E.; Schreiber, R.; Kemmler, M.; Mayer, H. A.; Fawzi, R.; Steimann, M. *Z. Anorg. Allg. Chem.* **1993**, *619*, 202.

(24) (a) Anderson, G. K.; Kumar, R. *Inorg. Chim. Acta* **1988**, *146*, 89. (b) Morvillo, A.; Bressan, M. *Inorg. Chim. Acta* **1986**, *121*, 219. (c) Bressan, M.; Morandini, F.; Rigo, P. *Inorg. Chim. Acta* **1983**, *77*, L139.

(25) Appleton, T. G.; Clark, H. C.; Manzer, L. E. *Coord. Chem. Rev.* **1973**, *10*, 335.

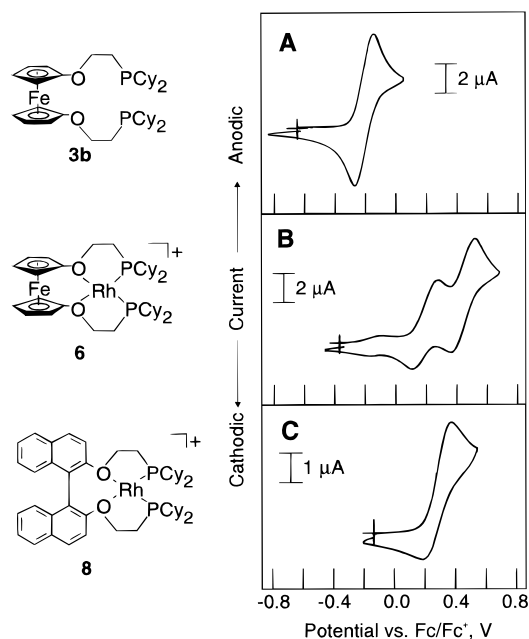
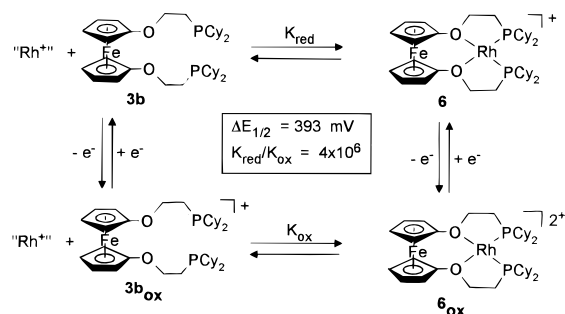


**Figure 5.** Cyclic voltammograms measured in  $\text{CH}_2\text{Cl}_2/0.1 \text{ M } ^n\text{Bu}_4\text{-PF}_6$  for (A) **3b** at 200 mV/s at a 1 mm diameter glassy carbon disk electrode, (B) **6** at 200 mV/s at a 1 mm diameter glassy carbon disk electrode, and (C) **8** at 50 mV/s at a 1.6 mm diameter Pt disk electrode.

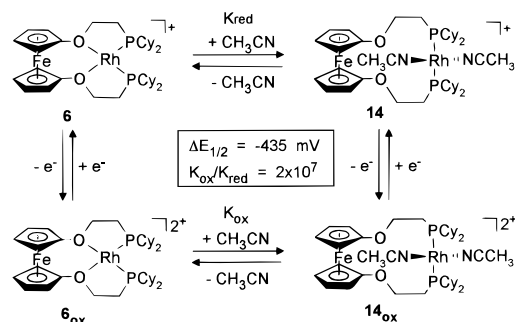
over the phenyl groups, which should favor the *trans* ligand arrangement. Interestingly, in the presence of 4 equiv of MeCN, **6** remains intact as judged by the absence of any resonances in the  $^{31}\text{P}$  NMR except those of **6**, indicating that the reaction is indeed an equilibrium. Likewise, in the presence of 2.5 equiv of MeCN, **5** does not completely react, and a mixture of **5**, **12**, and **13** is observed by  $^{31}\text{P}$  NMR spectroscopy. In contrast to the Rh–O linkages of **5** and **6**, the Rh–S linkages of **9** are relatively strong bonds and, according to  $^{31}\text{P}$  NMR spectroscopy, are not displaced by MeCN.

**Demonstration of the RHL Effect.** Cyclic voltammetry has been employed as a probe of the charge dependent binding ability of the RHLs in this study. Ligand **3b** exhibits a reversible oxidation/reduction wave at  $-200 \text{ mV}$  vs  $\text{Fc}/\text{Fc}^+$ , which reflects the strong  $\pi$ -donating properties of the ether substituents, Figure 5A. Upon **3b**'s complexation of Rh to form **6**, its  $E_{1/2}$  shifts  $+393 \text{ mV}$ , and a second reversible process is observed at higher potential ( $442 \text{ mV}$  vs  $\text{Fc}/\text{Fc}^+$ ), Figure 5B. The latter wave is assigned to a Rh (I/II) redox couple. The assignments are supported by data from model complex **8**, which contains Rh in a similar ligand environment but has no redox-active ligand and still undergoes a quasi-reversible redox process at  $299 \text{ mV}$  vs  $\text{Fc}/\text{Fc}^+$ , Figure 5C. The pronounced shift in the  $E_{1/2}$  of **6** compared to **3b** ( $393 \text{ mV}$ ) may be attributed to inductive withdrawal of electron density from the ferrocenyl group by the cationic Rh center as well as electrostatic repulsion between the formally cationic Rh(I) and Fe(III) centers. The magnitude of this shift in  $E_{1/2}$  can be used to calculate the ratio of the Rh(I) binding constants for reduced and oxidized **3b**; this is essentially a measure of the "RHL effect" or the increased lability of the ether moieties upon oxidation of **6**. The binding constant for **3b** in the reduced and oxidized states is defined in the square wave diagram of Scheme 4. Using this diagram and the Nernst equation, the ratio of ligand binding constants between the reduced and oxidized forms of **6** may be determined. In practice, one cannot measure the  $E_{1/2}$  of **3b** in the presence of dissociated "Rh $^{+}$ " but the  $E_{1/2}$  of **3b** is a reasonable approximation. Thus

#### Scheme 4



#### Scheme 5



$$\begin{aligned} \Delta E_{1/2} &= E_{1/2}(\mathbf{6}) - E_{1/2}(\mathbf{3b}) = -(RT/nF) \ln \left( \frac{[\mathbf{6}_{\text{ox}}]/[\mathbf{6}]}{[\mathbf{3b}_{\text{ox}}]/[\mathbf{3b}]} \right) \\ &= -(RT/nF) \ln \left( \frac{[\mathbf{6}_{\text{ox}}]/[\mathbf{6}]}{[\mathbf{3b}_{\text{ox}}]/[\mathbf{3b}]} \right) \\ &= (RT/nF) \ln \left( \frac{[\mathbf{6}]/[\mathbf{3b}]}{[\mathbf{6}_{\text{ox}}]/[\mathbf{3b}_{\text{ox}}]} \right) \\ &= (RT/nF) \ln(K_{\text{red}}/K_{\text{ox}}) \end{aligned}$$

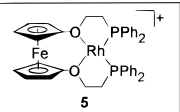
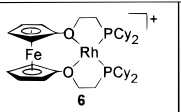
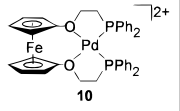
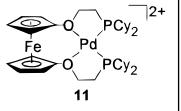
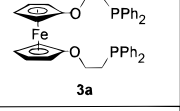
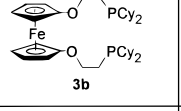
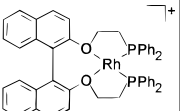
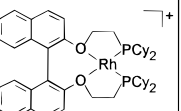
The  $\Delta E_{1/2}$  between **3b** and **6** is  $393 \text{ mV}$ , which corresponds to  $(K_{\text{red}}/K_{\text{ox}}) = 4.43 \times 10^6$ . Ligand based oxidation, thus, leads to a substantial change in ligand binding affinity and should, correspondingly, affect the reactivity of the RHL metal complex, especially with regard to the substitutionally labile ether moieties.

Alternative to the above analysis, one can quantify the RHL effect by examining how the equilibrium between **6** and MeCN is affected by ligand oxidation. These values can be derived from the electrochemical behavior of **6** in the absence and presence of MeCN. The cyclic voltammetry of **6** in 10% MeCN/ $\text{CH}_2\text{Cl}_2/0.1 \text{ M } ^n\text{Bu}_4\text{NPF}_6$  solution is markedly different from **6** in  $\text{CH}_2\text{Cl}_2/0.1 \text{ M } ^n\text{Bu}_4\text{NPF}_6$  and is consistent with the formation of **14**, Scheme 5. A reversible wave at  $-235 \text{ mV}$  vs  $\text{Fc}/\text{Fc}^+$  is assigned to the ferrocenyl portion of the complex, which is no longer bound to the rhodium via the ethers and thus oxidizes at a lower potential. At higher potentials an irreversible wave is present at  $E_{\text{pa}} = 595 \text{ mV}$  vs  $\text{Fc}/\text{Fc}^+$  and is assigned to Rh(I) oxidation. From the shift in  $E_{1/2}$  ( $\Delta E_{1/2}$ ) associated with the ferrocenyl group before and after MeCN binding, one can determine a ratio of MeCN binding constants for oxidized and reduced **6** ( $K_{\text{ox}}/K_{\text{red}}$ ). Again, using a square wave diagram (Scheme 5), which relates the equilibria involving **6** and **6<sub>ox</sub>** with MeCN, one can derive from the Nernst equation the following relationship:

$$\Delta E_{1/2} = E_{1/2}(\mathbf{14}) - E_{1/2}(\mathbf{6}) = -(RT/nF) \ln(K_{\text{ox}}/K_{\text{red}})$$

For the reaction depicted in Scheme 5,  $\Delta E_{1/2} = -435 \text{ mV}$ , which corresponds to a  $K_{\text{ox}}/K_{\text{red}}$  ratio of  $2.27 \times 10^7$ , a substantial change based on merely oxidizing the RHL. This demonstration

**Table 3.** Electrochemical Behavior of RHL Complexes and Models<sup>a</sup>

	270 <sup>+</sup>		193
	420 <sup>+</sup>		388
	-203		-200
	505 <sup>+</sup>		299

<sup>a</sup> Cyclic voltammetry results ( $E_{1/2}$  (mV vs Fc/Fc<sup>+</sup>), except where noted) for a series of RHL complexes and models. Data recorded from solutions of 0.1 M <sup>n</sup>Bu<sub>4</sub>NPF<sub>6</sub> in CH<sub>2</sub>Cl<sub>2</sub>. \* $E_{pa}$ : appears irreversible at moderate scan rates (<1 V/s).

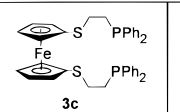
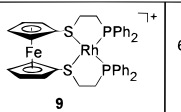
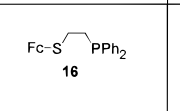
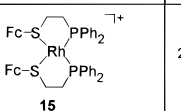
clearly shows how coordination sites on a transition metal can be *selectively* controlled via the RHL approach.

**Factors Controlling RHL Behavior and Maximizing the RHL Effect.** To develop an understanding of the fundamental factors that control the behavior of RHL complexes and to learn how to maximize the RHL effect, a series of RHL complexes was studied via cyclic voltammetry, Table 3. To determine the dependence of the central metal's valency upon the stability of the RHL system, Pd(II) complex **11** was prepared, and its electrochemical behavior was compared with the Rh(I) analogue **6**, Table 3. A strong correlation exists between the valency of the central metal and the  $E_{1/2}$  of the RHL complex. Replacement of Rh(I) with Pd(II) results in a 195 mV increase in the  $E_{1/2}$  for complexes of this type, Table 3. As a square planar d<sup>8</sup> complex, **11** has a very similar structure to **6**; the rigidity of the ligand imposes this geometrical constraint, as was verified in the crystal structures of **5**, **10**, and **11**. With the Fe–M distance fixed in this set of complexes, the  $E_{1/2}$  values of **6** and **11** suggest the role of inductive withdrawal and possibly electrostatic effects in the destabilization of RHL metal complexes but does not indicate the relative importance of these factors.

Upon moving from its reduced to oxidized states, palladium complex **11** provides a greater change in stability than the analogous electrochemical reaction involving **6**. A square wave diagram analysis, as performed with **6** in Scheme 4, reveals a  $K_{red}/K_{ox}$  of  $8.6 \times 10^9$ , which is an increase of three orders of magnitude over the analogous ratio involving **6**. Thus, increasing the formal charge on the metal leads to substantial enhancement of the charge dependent properties of this class of RHL metal complexes.

The phosphine substituents of RHLs offer another potential method for controlling or tuning the behavior of RHL complexes. Electron donating groups are expected to "soften" bound transition metal centers over electron withdrawing groups. Indeed, the phenyl substituted complexes **5** and **10** have very different electrochemical behavior from their cyclohexyl analogues. The trend of central metal valency and complex stability elucidated for **6** and **11** applies to **5** and **10** as well, Table 3. With phenyl substituted complexes, however, the cyclic voltammograms are irreversible at moderate scan rates (0.2–1 V/sec), which is a reflection of the instability of the oxidized forms of

**Table 4.** Electrochemical Behavior of Redox-Active Thioether Complexes and Ligands<sup>a</sup>

	37		677
	35		245

<sup>a</sup> Fc = ( $\eta^5$ -C<sub>5</sub>H<sub>5</sub>)Fe( $\eta^5$ -C<sub>5</sub>H<sub>4</sub>)<sup>-</sup>. Cyclic voltammetry results ( $E_{1/2}$  (mV vs Fc/Fc<sup>+</sup>)) recorded from 0.1 M <sup>n</sup>Bu<sub>4</sub>NPF<sub>6</sub> in CH<sub>2</sub>Cl<sub>2</sub>.

these compounds. At present, the decomposition products are unknown. The disparity in the behavior of RHL complexes with phenyl phosphines (**5** and **10**) and cyclohexyl phosphines (**6** and **11**) shows how one cannot only tune the electronic nature of the RHLs but also the stability of the oxidized form of the bound transition metals. This is further verified by examination of the electrochemical behavior of model complexes **7** and **8**. These complexes contain Rh in a similar electronic environment to **5** and **6**, but the redox-active ferrocenyl groups have been replaced with the redox-inactive binaphthyl groups (Table 3). Cyclic voltammetry of these complexes allows one to directly evaluate the electronic nature of the bound Rh center. Compound **7** undergoes an irreversible oxidation at 505 mV vs Fc/Fc<sup>+</sup>, while **8**, with cyclohexyl phosphines, undergoes a quasi-reversible redox process at 299 mV vs Fc/Fc<sup>+</sup>. The large potential difference of these complexes reflects the increased electron donating properties of the cyclohexyl groups as compared with phenyl groups. Significantly, however, *the cyclohexyl electron donating effects are not so large as to limit the "RHL-effect", and substantial differences in reactivity occur between 6 and its oxidized form.* This has been demonstrated by analysis of the equilibrium reactions of MeCN with both **6** and **6<sub>ox</sub>** (*vide supra*).

To further control the behavior of RHL complexes, the labile binding group can be synthetically altered. As was demonstrated in the reactivity studies, thioether RHLs offer stronger binding to Rh. Both bidentate<sup>1</sup> and tetradentate phosphine thioether ligands have been studied and complexed to Rh(I). Comparison of their electrochemical behaviors (Table 4) illustrates the role of electrostatics in the destabilization of RHL complexes. Complex **15**, which is formed from the bidentate ligand **16**, exhibits two reversible ferrocenyl based oxidation/reduction waves at 225 and 440 mV vs Fc/Fc<sup>+</sup>. For comparison with complex **9** (formed from tetradentate **3c**) the first wave will be considered. At scan rates less than or equal to 1 V/s, **9** undergoes an irreversible oxidation at  $E_{pa} = 550$  mV vs Fc/Fc<sup>+</sup>, consistent with the electrochemical behavior of other tetradentate RHL complexes with phenyl phosphines, which degrade upon oxidation. At 100 V/s, however, a reversible wave for **9** has been observed at 677 mV vs Fc/Fc<sup>+</sup>. To investigate the role of electrostatic interactions in the destabilization of the oxidized forms of these complexes, the ratio of ligand binding constants for Rh(I) in each RHL's reduced and oxidized states was determined. These values reflect the change in thioether binding strength that results from ligand oxidation. The tetradentate complex exhibits a shift ( $K_{red}/K_{ox} = 1.27 \times 10^{11}$ ) much more than double that of the bidentate complex ( $K_{red}/K_{ox} = 3.87 \times 10^3$ ). To a first approximation, the inductive effects that result from Rh binding in **9** should be no greater than double the inductive withdrawal from the ferrocenyl groups in **15**. Both complexes contain similar thioether binding groups on ferrocene; for **15** each ferrocenyl group is monosubstituted, while the

**Table 5.** Crystallographic Data for 5, 9, 10, and 11

	5	9	10	11
formula	C <sub>42</sub> H <sub>44</sub> O <sub>3</sub> P <sub>2</sub> FeRhBF <sub>4</sub>	C <sub>40</sub> H <sub>40</sub> BF <sub>4</sub> FeO <sub>0.5</sub> P <sub>2</sub> RhS <sub>2</sub>	C <sub>38.6</sub> H <sub>37.2</sub> B <sub>2</sub> Cl <sub>1.2</sub> F <sub>8</sub> FeO <sub>2</sub> P <sub>2</sub> Pd	C <sub>38</sub> H <sub>60</sub> B <sub>2</sub> F <sub>8</sub> FeO <sub>2</sub> P <sub>2</sub> Pd
formula weight	904.31	900.35	973.43	946.67
space group	P2 <sub>1</sub> 2 <sub>1</sub> 2 <sub>1</sub>	P2 <sub>1</sub> /n	P2 <sub>1</sub> /c	P2 <sub>1</sub> /c
a, Å	9.838(2)	12.252(2)	14.653(2)	10.638(2)
b, Å	17.799(6)	20.884(4)	20.987(2)	17.011(3)
c, Å	21.939(4)	17.140(3)	15.441(2)	29.978(4)
β, deg		110.03(1)	103.41(1)	97.92(1)
V, Å <sup>3</sup>	3842(3)	4120(1)	4619(1)	4119(1)
Z	4	4	4	4
crystal color	orange plate	reddish-brown plate	brown plate	red thin plate
D(calc), g cm <sup>-3</sup>	1.563	1.451	1.400	1.527
μ(Mo Kα), cm <sup>-1</sup>	9.44	9.78	9.04	9.36
temp, K	153(1)	298(2)	298(2)	247(2)
diffractometer	Enraf-Nonius CAD-4	Siemens P4	Siemens P4	Siemens P4
radiation			MoKα (λ = 0.71073 Å)	
R(F), %	4.8 <sup>a</sup>	6.35 <sup>b</sup>	7.22 <sup>b</sup>	4.65 <sup>b</sup>
R(wF <sup>2</sup> ), %	4.4 <sup>a</sup>	15.32 <sup>b,c</sup>	16.43 <sup>b,c</sup>	8.99 <sup>b,c</sup>

<sup>a</sup> Quantity minimized =  $\sum w\Delta^2$ ;  $R = \sum \Delta / \sum (F_o)$ ;  $R(w) = \sum \Delta w^{1/2} / \sum (F_o w^{1/2})$ ,  $\Delta = |(F_o - F_c)|$ . <sup>b</sup> Quantity minimized =  $R = \sum \Delta / \sum (F_o)$ ,  $\Delta = |(F_o - F_c)|$ ;  $R(wF^2) = \sum [w(F_o^2 - F_c^2)^2] / \sum [w(F_o^2)^2]^{1/2}$ . <sup>c</sup>  $R(wF^2)$ , %.

ferrocenyl group in **9** bears two thioether substituents. The main difference between **9** and **15** is the geometric constraint in **9** imposed by the tetradentate ligand. As a result the Rh–Fe separation in **9** is fixed and significantly shorter (4.055(7) Å) than that of **15** (~5.2 Å). Due to this geometry, the contribution of electrostatic repulsion in the destabilization of our tetradentate RHL complexes should be larger than in similar bidentate complexes. While the absolute contribution of electrostatic repulsion cannot be directly extracted from these experiments, in this study, cyclic voltammetry and the determined binding constant ratios indicate that electrostatic repulsion significantly contributes to the destabilization of the RHL systems upon their oxidation.

## Conclusions

Tetradentate redox-switchable hemilabile ligands (RHLs) offer tremendous control over ligand binding affinity and thus the reactivity of a bound metal center through electrochemically induced changes in ligand binding strengths. These changes can be substantial (~10<sup>11</sup>) and vary according to the transition metal, transition metal valency, position of the redox group within the complex, and the type of ancillary ligands. For Rh(I) complex **6**, ligand based oxidation weakens the Rh–O bonds and results in an increase in the equilibrium constant for the reaction of **6** with MeCN such that  $K_{ox}/K_{red} = 2.27 \times 10^7$ . The Pd(II) complex, **11**, exhibits a greater change in ligand binding strength upon oxidation than the Rh(I) complex, **6**. This trend of bound metal valency and change in RHL complex stability is also present in complexes **5** and **10**, with phenyl phosphines instead of cyclohexyl phosphines. However, the electrochemical behavior of each tetradentate phenyl-substituted RHL–metal complex in this study is irreversible at moderate to slow scan rates. Thus, phosphine substituents offer a high degree of tunability over the stability of RHL complexes. Cyclohexyl groups electronically soften and stabilize the metal complexes without significantly altering the charge-dependent changes in reactivity. Thioether RHLs have been synthesized and offer increased binding strength to Rh(I) compared to ether RHLs. Comparison of the electrochemical responses of thioether complexes **9** and **15** has implicated electrostatic repulsion as a significant factor in the destabilization of RHL complexes, at least for the metals and ligands chosen in this study. This is in spite of the ability of transition metals to delocalize their charge upon ancillary ligands, which could, in other systems, substantially decrease their charge densities.

## Experimental Section

Unless otherwise noted, all reactions were carried out under inert conditions using standard Schlenk techniques. Tetrahydrofuran (THF) and diethyl ether (Et<sub>2</sub>O) were dried and distilled over sodium-benzophenone. Pentane, methylene chloride, and acetonitrile were dried and distilled from calcium hydride. Acetone was doubly distilled over potassium carbonate. <sup>1</sup>H and <sup>31</sup>P NMR spectra were recorded on either a Varian Gemini 300 MHz, a Varian VXR 300 MHz, or a Varian Unity 400 MHz FT-NMR spectrometer. The <sup>31</sup>P chemical shifts were measured relative to external 85% H<sub>3</sub>PO<sub>4</sub>. X-ray crystallography was performed on either an Enraf-Nonius CAD-4 (**5**) or a Siemens P4 diffractometer (**9–11**). Electrochemical measurements were carried out on either a PINE AFRDE4 or AFRDE5 bipotentiostat or a PAR 273A potentiostat/galvanostat using Au, Pt, or glassy carbon disk electrodes with a Pt mesh counter electrode and an Ag wire reference electrode. Fast voltammetry was performed on a custom built high scan rate potentiostat in the laboratory of Professor F. G. Bordwell of Northwestern University. For each electrochemical experiment the supporting electrolyte was 0.1 M <sup>n</sup>Bu<sub>4</sub>PF<sub>6</sub> in CH<sub>2</sub>Cl<sub>2</sub>. All electrochemical data were referenced versus the internal standard: ferrocene/ferrocenium redox couple or decamethylferrocene/decamethylferrocenium. Fast atom bombardment (FAB) and electron ionization (EI) mass spectra were recorded on a Fisons VG 70–250 SE mass spectrometer. Trifluoromethane sulfonic anhydride, methyl lithium, butyllithium, 2-hydroxyethyl disulfide, potassium diphenylphosphide, and silver tetrafluoroborate were used as received from Aldrich Chemical Co. Thionyl chloride was purchased from Fisher Scientific and used without further purification. Dicyclohexylphosphine and tetrakis(acetonitrile)palladium(II) tetrafluoroborate were used as received from Strem Chemicals Inc. RhCl<sub>3</sub>·xH<sub>2</sub>O was used on loan from Johnson-Matthey Chemical Company. [Rh(μ-Cl)(η<sup>2</sup>-C<sub>8</sub>H<sub>14</sub>)<sub>2</sub>]<sub>2</sub>,<sup>26</sup> [Rh(μ-Cl)(η<sup>2</sup>-C<sub>2</sub>H<sub>4</sub>)<sub>2</sub>]<sub>2</sub>,<sup>27</sup> 1,1'-ferrocenylene diacetate,<sup>9</sup> and 2,2'-bis(2-chloroethoxy)-1,1'-binaphthalene<sup>16</sup> were prepared according to literature methods.

**Syntheses. 1,1'-Bis(2-chloroethoxy)ferrocene.** A mixture of ferrocenylene diacetate (1.215 g, 0.00402 mol) in 75 mL of diethyl ether was cooled to –78 °C. A 1.4 M solution of methyl lithium in Et<sub>2</sub>O (12.3 mL, 0.0172 mol) was added to the mixture through an addition funnel. After 15 min a yellow-orange suspension formed, which was cooled to –78 °C and added via cannula to a solution of 2-chloroethyltrifluoromethane sulfonate<sup>11</sup> (3.73 g, 0.0186 mol) at –78 °C. The resulting orange mixture was warmed and heated at reflux (35 °C) for 14 h. After washing with 2% NaOH solution and saturated NaCl solution in water, the orange organic layer was dried over MgSO<sub>4</sub> and the solvent was removed by rotary evaporation. Column chromatography on silica gel with 20% ethyl acetate/80% hexane as an eluent gave an orange band, which upon removal of solvent yielded an orange

(26) Porri, L.; Lionetti, A.; Allegra, G.; Immirizi, A. *J. Chem. Soc., Chem. Commun.* **1965**, 336.

(27) Cramer, R. *Inorg. Chem.* **1962**, *1*, 722.



solid product (1.072 g, 78%). Analytically pure samples were obtained via recrystallization from ethanol.  $^1\text{H NMR}$  ( $\text{C}_6\text{D}_6$ ):  $\delta$  3.97 (m, Fc protons, 4H), 3.72 (m, Fc protons, 4H), 3.59 (t,  $\text{OCH}_2$ ,  $J_{\text{H-H}} = 5.5$  Hz, 4H), 3.22 (t,  $\text{CH}_2\text{Cl}$ ,  $J_{\text{H-H}} = 5.5$  Hz, 4H). HREIMS [ $M^+$ ]: Calcd,  $m/z$  341.9877; found,  $m/z$  341.9872. Anal. Calcd for  $\text{C}_{14}\text{H}_{16}\text{O}_2\text{Cl}_2\text{Fe}$ : C, 49.02; H, 4.70. Found: C, 48.87; H, 4.78.

**1,1'-Bis(2-diphenylphosphinoethoxy)ferrocene (3a).** A 0.5 M solution of potassium diphenylphosphide (3.4 mL, 1.7 mmol) in THF was diluted with 50 mL of THF and cooled to  $-10$  °C. A solution of 1,1'-bis(2-chloroethoxy)ferrocene (0.14 g, 0.41 mmol) in THF was added dropwise to the mixture through an addition funnel. The mixture was slowly warmed to room temperature and stirred overnight. The resulting orange solution contained a white precipitate, which presumably was KCl. An  $\text{Et}_2\text{O}/\text{H}_2\text{O}$  extraction provided an orange-yellow organic layer which was dried over  $\text{MgSO}_4$  and evaporated to an orange oil. Column chromatography in a glovebox (silica gel, benzene eluent) and recrystallization from ethanol provided an orange microcrystalline product (0.25 g, 96%).  $^1\text{H NMR}$  ( $\text{C}_6\text{D}_6$ ):  $\delta$  7.44 (m, Ph, 8H), 7.06 (m, Ph, 12H), 3.92 (m, Fc protons and  $\text{OCH}_2$ , 8H), 3.66 (m, Fc protons, 4H), 2.46 (t,  $\text{CH}_2\text{P}$ ,  $J_{\text{H-H}} = 7.9$  Hz, 4H).  $^{31}\text{P}\{^1\text{H}\}$  NMR ( $\text{C}_6\text{D}_6$ ):  $\delta$  21.9 (s). HRFABMS [ $M^+$ ]: Calcd,  $m/z$  642.1540; found:  $m/z$  642.1529. Anal. Calcd for  $\text{C}_{38}\text{H}_{36}\text{FeO}_2\text{P}_2$ : C, 71.04; H, 5.65. Found: C, 70.45; H, 5.75.

**1,1'-Bis(2-dicyclohexylphosphinoethoxy)ferrocene (3b).** A 2.0 M pentane solution of butyllithium (0.9 mL, 1.78 mmol) was added to a colorless solution of dicyclohexylphosphine (0.32 mL, 1.58 mmol) in 15 mL of THF at 0 °C. After 50 min the resulting orange solution was added dropwise to a solution of 1,1'-(2-chloroethoxy)ferrocene (252 mg, 0.74 mmol) in 20–25 mL of THF at 0 °C. After 8 h of slowly warming to room temperature the orange reaction mixture was evaporated onto alumina (predried at 0.02 mm Hg) and chromatographed in a glovebox with 1:4 diethyl ether/pentane to yield a pure orange oil (293 mg, 60%).  $^1\text{H NMR}$  ( $\text{CDCl}_3$ ):  $\delta$  4.05 (dd,  $J_{\text{H-H}} = 1.9$  Hz, 4H, Fc); 3.86 (m, 4H,  $\text{CH}_2\text{O}$ ); 3.81 (dd,  $J_{\text{H-H}} = 1.9$  Hz, 4H, Fc); 1.86–1.62 (m, 24H,  $\text{CH}_2\text{P}$  and cyclohexyl); 1.56 (m, 4H, ring *CHP*); 1.35–1.05 (m, 20H, cyclohexyl).  $^{31}\text{P}\{^1\text{H}\}$  NMR ( $\text{CDCl}_3$ ):  $\delta$  -11.1 (s). HREIMS [ $M^+$ ]: Calcd,  $m/z$  666.3418; found,  $m/z$  666.3419. Anal. Calcd for  $\text{C}_{38}\text{H}_{60}\text{FeO}_2\text{P}_2$ : C, 68.46; H, 9.07. Found: C, 68.62; H, 9.14.

**2-Chloroethyldisulfide.** This reaction was not carried out under airfree conditions. Pyridine (5.3 mL, 0.064 mol) was added via syringe to a 40 mL THF solution of 2-hydroxyethyldisulfide (2.0 mL, 0.016 mol) and thionyl chloride (4.8 mL, 0.064 mol). The resulting mixture developed white and yellow precipitates as it became warm. After 18 h the reaction mixture was treated with water and extracted with ether. Drying over  $\text{Na}_2\text{SO}_4$  and removal of solvent provided a clean orange brown liquid (2.54 g, 83%). Precipitates from the reaction mixture were soluble in the aqueous layer, which was orange.  $^1\text{H NMR}$  ( $\text{CDCl}_3$ ):  $\delta$  3.75 (t,  $J_{\text{H-H}} = 7.5$  Hz, 4H,  $\text{CH}_2\text{Cl}$ ); 3.00 (t,  $J_{\text{H-H}} = 7.5$  Hz, 4H,  $\text{CH}_2\text{S}$ ).

**1,1'-Bis(2-chloroethylthio)ferrocene.** To a solution of *N,N,N',N'*-tetramethylethylenediamine (1.6 mL, 10.6 mmol) in 20 mL of hexane was added 2.0 M butyllithium in pentane (5.25 mL, 10.5 mmol). A white precipitate developed below the pale yellow solution. Upon slow addition of a saturated solution of ferrocene (0.974 g, 5.24 mmol) in hexane an orange precipitate formed. After  $3\frac{1}{2}$  h of stirring the reaction mixture was cooled to 0 °C and diluted to 80 mL. 2-Chloroethyldisulfide (2.08 g, 10.9 mmol) was added via syringe, and the reaction mixture became brown as it was stirred overnight and warmed to room temperature. Following an aqueous/ether extraction and drying over  $\text{MgSO}_4$ , the crude product was chromatographed on silica with 5% ether in hexane. The product was isolated as an orange solid upon removal of solvent (259 mg, 13%). A significant quantity of ferrocene was recovered from the reaction product mixture.  $^1\text{H NMR}$  ( $\text{CDCl}_3$ ):  $\delta$  4.31 (dd,  $J_{\text{H-H}} = 1.8$  Hz, 4H, Fc); 4.25 (dd,  $J_{\text{H-H}} = 1.8$  Hz, 4H, Fc); 3.52 (t,  $J_{\text{H-H}} = 8.0$  Hz, 4H,  $\text{CH}_2\text{Cl}$ ); 2.83 (t,  $J_{\text{H-H}} = 8.0$  Hz,  $\text{CH}_2\text{S}$ ). HREIMS [ $M^+$ ]: Calcd,  $m/z$  373.9420; found:  $m/z$  373.9416. Anal. Calcd for  $\text{C}_{38}\text{H}_{36}\text{FeP}_2\text{S}_2$ : C, 67.66; H, 5.38. Found: C, 67.02; H, 5.46.

**1,1'-Bis(2-diphenylphosphinoethylthio)ferrocene (3c).** Potassium diphenylphosphide solution (2.6 mL of 0.5 M in THF, 1.3 mmol) was added dropwise to a solution of 1,1'-bis(2-chloroethylthio)ferrocene (212 mg, 0.56 mmol) in 15 mL of THF, cooled to 0 °C. After 12 h and warming to room temperature the reaction mixture was evaporated onto

silica and chromatographed in a glovebox. After treatment with 10%  $\text{Et}_2\text{O}$  in hexane to remove  $\text{HPPH}_2$ , THF was used to elute the product, which was isolated as yellow-orange solid (189 mg, 50%).  $^1\text{H NMR}$  ( $\text{CDCl}_3$ ):  $\delta$  4.26 (dd,  $J_{\text{H-H}} = 1.9$  Hz, 4H, Fc); 4.21 (dd,  $J_{\text{H-H}} = 1.9$  Hz, 4H, Fc); 2.60 (m, 4H,  $\text{CH}_2\text{S}$ ); 2.25 (m, 4H,  $\text{CH}_2\text{P}$ ).  $^{31}\text{P}\{^1\text{H}\}$  NMR ( $\text{CDCl}_3$ ):  $\delta$  -16.6 (s). FABMS [ $M^+$ ]:  $m/z$  674. Anal. Calcd for  $\text{C}_{38}\text{H}_{36}\text{FeS}_2\text{P}_2$ : C, 67.66; H, 5.38. Found: C, 67.02; H, 5.46.

**2,2'-Bis(2-dicyclohexylphosphinoethoxy)-1,1'-binaphthalene (4b).** A 2.0 M solution of butyllithium in pentane (0.9 mL, 1.8 mmol) was added to a 15 mL THF solution of dicyclohexylphosphine (0.31 mL, 1.53 mmol) cooled to 0 °C. The resulting solution turned yellow-orange over 1 h, at which time it was transferred dropwise to a 30 mL THF solution of 2,2'-bis(2-chloroethoxy)-1,1'-binaphthalene at 0 °C. The clear solution was stirred for 10 h at 0 °C and 10 h at  $-78$  °C. It was directly chromatographed on alumina with 1:9 diethyl ether/pentane in a glovebox to yield a colorless oil (271 mg, 50%), which was stored at  $-40$  °C in a glovebox freezer.  $^1\text{H NMR}$  ( $\text{CDCl}_3$ ):  $\delta$  8.0–7.8 (m, 4H, aromatic); 7.5–7.0 (m, 4H, aromatic); 4.1 (m, 6H,  $\text{CH}_2$ ); 3.36 (t,  $J_{\text{H-H}} = 6.5$  Hz, 2H,  $\text{CH}_2$ ); 1.8–0.9 (m, 44H, cyclohexyl).  $^{31}\text{P}\{^1\text{H}\}$  NMR ( $\text{CDCl}_3$ ):  $\delta$  -10.9 (s). HRFABMS [ $M^+\cdot\text{H}^+$ ]: Calcd,  $m/z$  735.4460; found,  $m/z$  735.4474.

**Rhodium(I) [1,1'-Bis(2-diphenylphosphinoethoxy)ferrocene]tetrafluoroborate (5).** In a typical preparation ( $\eta^2\text{-CH}_2\text{CH}_2$ ) $\text{Rh}_2(\mu\text{-Cl})_2$  (71.4 mg, 0.184 mmol) and  $\text{AgBF}_4$  (72 mg, 0.37 mmol) were mixed as solids. Upon addition of 3–5 mL of THF a cloudy mixture immediately formed. After stirring for 45 min a gray-black precipitate was filtered off through Celite leaving an orange filtrate, which was diluted (150 mL THF) and cooled to  $-40$  °C. A solution of 1,1'-bis(2-diphenylphosphinoethoxy)ferrocene (3a) (236 mg, 0.367 mmol) in 25 mL THF was added dropwise via an addition funnel over 20 min. After stirring for 1 h, the orange solution was warmed to room temperature and the solvent removed *in vacuo*, yielding 5 as an orange powder (spectroscopic yield > 95%). Single crystals of 5 were obtained by slow diffusion of pentane into a THF solution of the product.  $^1\text{H NMR}$  ( $\text{CD}_2\text{Cl}_2$ ):  $\delta$  7.5–7.2 (m, Ph, 20H); 4.75 (m, Fc protons, 4H); 4.10 (m, Fc protons, 4H); 3.75 (m,  $\text{CH}_2\text{O}$ , 4H); 3.69 (m, THF, 4H), 2.62 (m,  $\text{CH}_2\text{P}$ , 4H), 1.83 (m, THF, 4H).  $^{31}\text{P}\{^1\text{H}\}$  NMR ( $\text{CD}_2\text{Cl}_2$ ):  $\delta$  61.1 (d,  $J_{\text{Rh-P}} = 210$  Hz). HRFABMS [ $M^+$ ]: Calcd,  $m/z$  745.0595; found:  $m/z$  745.0623.

**Rhodium(I) [1,1'-(2-Dicyclohexylphosphinoethoxy)ferrocene]tetrafluoroborate (6).** A mixture of  $[\text{RhCl}(\text{C}_8\text{H}_{14})_2]_x$  (53.5 mg, 0.15 mmol),  $\text{AgBF}_4$  (29 mg, 0.15 mmol), and 3 mL of THF was stirred for 1 h. After filtration through Celite the resulting orange filtrate was diluted to 50 mL with THF and cooled to  $-40$  °C. A 3 mL THF solution of 1,1'-(2-dicyclohexylphosphinoethoxy)ferrocene (3b) (100 mg, 0.15 mmol) was added dropwise. The orange reaction solution was stirred for 1 h and then concentrated *in vacuo*. Upon addition of excess hexane a pure orange powder precipitated from solution (71 mg, 55%).  $^1\text{H NMR}$  ( $\text{CD}_2\text{Cl}_2$ ):  $\delta$  4.63 (dd,  $J_{\text{H-H}} = 2.0$  Hz, 4H, Fc); 4.04 (dd,  $J_{\text{H-H}} = 2.0$  Hz, 4H, Fc); 3.92 (dt, 4H,  $J_{\text{H-H}} = 6.6$  Hz,  $J_{\text{H-P}} = 16.5$  Hz,  $\text{CH}_2\text{O}$ ); 2.44 (m, 4H, ring *CHP*); 2.1–1.2 (m, 44H,  $\text{CH}_2\text{P}$  and Cy).  $^{31}\text{P}\{^1\text{H}\}$  NMR ( $\text{CD}_2\text{Cl}_2$ ):  $\delta$  68.3 (d,  $J_{\text{Rh-P}} = 203$  Hz). FABMS [ $M^+$ ]:  $m/z$  769.

**Rhodium(I) [2,2'-Bis(2-dicyclohexylphosphinoethoxy)-1,1'-binaphthalene]tetrafluoroborate (8).** A 4 mL portion of THF was added to a mixture of  $[\text{RhCl}(\text{C}_8\text{H}_{14})_2]_x$  (27 mg, 0.075 mmol) and  $\text{AgBF}_4$  (16 mg, 0.08 mmol) at room temperature. After 30 min a gray-black precipitate was filtered away, and the orange filtrate was diluted to 75 mL and cooled to  $-78$  °C. Following slow addition of a THF solution of 2,2'-bis(2-dicyclohexylphosphinoethoxy)-1,1'-binaphthalene]tetrafluoroborate (4b) (55 mg, 0.075 mmol) the reaction mixture was stirred for 2 h, while warming to  $-10$  °C. The solution was concentrated *in vacuo* to 7 mL at  $< -10$  °C, and the product precipitated after addition of 35 mL pentane. The product was purified via slow precipitation from a pentane/dichloromethane mixture to yield 33 mg (48%) of orange solid. When stored for periods longer than 2 h, the product was cooled to  $\leq -40$  °C.  $^{31}\text{P}\{^1\text{H}\}$  NMR ( $\text{CD}_2\text{Cl}_2$ ):  $\delta$  72.6 (d,  $J_{\text{Rh-P}} = 203$  Hz). FABMS [ $M^+$ ]:  $m/z$  837.

**Rhodium(I) [1,1'-Bis(2-diphenylphosphinoethylthio)ferrocene]tetrafluoroborate (9).** A mixture of  $[\text{RhCl}(\text{C}_8\text{H}_{14})_2]_x$  (27.3 mg, 0.076 mmol),  $\text{AgBF}_4$  (15 mg, 0.077 mmol), and 5 mL of THF was stirred for 45 min. After filtration of a grey precipitate through Celite, the

resulting orange filtrate was diluted to 60 mL with THF and cooled to  $-40\text{ }^{\circ}\text{C}$ . A 15 mL THF solution of 1,1'-bis(2-diphenylphosphinoethylthio)ferrocene (**3c**) was added dropwise to the reaction solution and stirred for 45 min. The orange solution was concentrated to 5 mL *in vacuo* at room temperature. Ether (50 mL) was added to precipitate the product as an orange brown residue (34 mg, 52%). Methylene chloride solutions of the product are brick red.  $^1\text{H}$  NMR ( $\text{CD}_2\text{Cl}_2$ ):  $\delta$  7.28 (m, 20H, Ph); 4.84 (m, 4H, Fc); 4.34 (m, 4H, Fc); 2.61 (m, 8H,  $\text{SCH}_2$  and  $\text{CH}_2\text{P}$ ).  $^{31}\text{P}\{^1\text{H}\}$  NMR ( $\text{CD}_2\text{Cl}_2$ ):  $\delta$  62.7 (d,  $J_{\text{Rh-P}} = 162$  Hz). FABMS [ $M^+$ ]:  $m/z$  777. Anal. Calcd for  $\text{C}_{38}\text{H}_{36}\text{FeRhS}_2\text{P}_2\text{BF}_4\cdot\text{C}_4\text{H}_8\text{O}$ : C, 53.87; H, 4.74. Found: C, 53.86; H, 4.58.

**Palladium(II) [1,1'-Bis(2-diphenylphosphinoethoxy)ferrocene]bis(tetrafluoroborate) (10)**. A solution of 1,1'-bis(2-diphenylphosphinoethoxy)ferrocene (**3a**) (42 mg, 0.065 mmol) in 25 mL of acetone was slowly transferred to a solution of palladium(II) tetrakis(acetonitrile) bis(tetrafluoroborate) (29 mg, 0.065 mmol) in 60 mL of acetone at  $-30\text{ }^{\circ}\text{C}$ . After 45 min the red-orange solution was concentrated to 5 mL and treated with hexanes (20 mL) to precipitate the product as a maroon residue (59 mg, 98%). Single crystals suitable for X-ray diffraction were grown by slow diffusion of pentane into methylene chloride solution.  $^1\text{H}$  NMR ( $\text{CD}_2\text{Cl}_2$ ):  $\delta$  7.68 (m, 8H, *o*-Ph); 7.59 (m, 4H, *p*-Ph); 7.47 (m, 8H, *m*-Ph); 5.22 (dd,  $J_{\text{H-H}} = 2.0$  Hz, 4H, Fc); 4.09 (dd,  $J_{\text{H-H}} = 2.0$  Hz, 4H, Fc); 3.89 (dt,  $J_{\text{H-H}} = 5.75$  Hz,  $J_{\text{H-P}} = 24.0$  Hz, 4H,  $\text{CH}_2\text{O}$ ); 3.29 (dt,  $J_{\text{H-H}} = 5.8$  Hz,  $J_{\text{H-P}} = 11.3$  Hz, 4H,  $\text{CH}_2\text{P}$ ).  $^{31}\text{P}\{^1\text{H}\}$  NMR ( $\text{CD}_2\text{Cl}_2$ ):  $\delta$  51.3 (s). FABMS [ $M^+$ ]:  $m/z$  748.

**Palladium(II) [1,1'-(2-Dicyclohexylphosphinoethoxy)ferrocene]bis(tetrafluoroborate) (11)**. Palladium(II) tetrakis(acetonitrile)bis(tetrafluoroborate) (25 mg, 0.056 mmol) was dissolved in 10 mL of acetone and cooled to  $-50\text{ }^{\circ}\text{C}$ . A solution of the 1,1'-(2-dicyclohexylphosphinoethoxy)ferrocene (**3b**) (35.9 mg, 0.054 mmol) was transferred dropwise, and the reaction mixture slowly turned from pale yellow to red. After 40 min the reaction mixture was warmed to room temperature, and the solvent was removed (spectroscopic yield >95%). Crystalline samples were obtained from slow diffusion of ether into a dichloromethane solution.  $^1\text{H}$  NMR (acetone- $d_6$ ):  $\delta$  5.01 (dd,  $J_{\text{H-H}} = 2.0$  Hz, 4H, Fc); 4.40 (dt,  $J_{\text{H-H}} = 6.5$  Hz,  $J_{\text{H-P}} = 18.1$  Hz, 4H,  $\text{CH}_2\text{O}$ ); 4.14 (dd,  $J_{\text{H-H}} = 2.0$  Hz, 4H, Fc); 3.03 (m, 4H, ring *CHP* or  $\text{CH}_2\text{P}$ ); 2.58 (m, 4H, ring *CHP* or  $\text{CH}_2\text{P}$ ); 2.2–1.2 (m, 40 H, Cy).  $^{31}\text{P}\{^1\text{H}\}$  NMR (acetone- $d_6$ ):  $\delta$  76.3 (s). FABMS [ $M^+$ ]: 772.

**Crystallographic Structural Determination.** Crystal, data collection, and refinement parameters are given in Table 5. Systematic absences in the diffraction data are uniquely consistent with the reported

space groups. The structures were solved using direct methods, completed by subsequent difference Fourier syntheses and refined by full-matrix, least-squares procedures. Semiempirical absorption corrections were applied. An extinction coefficient for **5** was refined and found to not be necessary. The fluorine atoms in one of the counterions in **11** are statistically disordered over two positions with an occupancy distribution of 60/40. A solvent molecule of tetrahydrofuran was located in **5** and **9**. The solvent of **9** has a refined occupancy of 50%. A solvent molecule of dichloromethane was located in **10** with a partial occupancy of 60%. Four peaks remained on the difference map of **10** for which no definitive chemical assignment could be made. These atoms were located near an inversion center, arbitrarily assigned carbon identities, and were refined isotropically. Two of these atoms were refined at full occupancy, and the other two were refined at 60% occupancy. The empirical formula for **10** and the intensive parameters calculated from it do not include these chemically unidentified atoms, although they are presumed to be highly disordered solvent molecules. The cyclopentadienyl and phenyl rings in **10** were fixed as rigid planar groups to conserve data. All other non-hydrogen atoms were refined with anisotropic displacement coefficients except for the solvent molecule in **5**, which was refined isotropically. Hydrogen atoms were treated as idealized contributions. Supporting Information contains further details on structural determinations.

All software and sources of the scattering factors are contained in either the SHELXTL PLUS (4.2) or the SHELXTL (5.3) program libraries (G. Sheldrick, Siemens XRD, Madison, WI).

**Acknowledgment.** We acknowledge the NSF (CHE-9625391 and CHE-9357099) for generously funding this research. We also thank Charlotte Stern for assistance in the structure determination of **5**. Professor F. G. Bordwell and Dr. Wei-Zhong Liu are acknowledged for assistance with fast voltammetry experiments.

**Supporting Information Available:** Detailed descriptions of the X-ray diffraction studies for **5**, **9**, **10**, and **11**, including tables of experimental details, atom positional parameters,  $B(\text{eq})$  values, bond lengths, bond angles, and anisotropic displacement parameters (44 pages). See any current masthead page for ordering and Internet access instructions.

JA963008A